JOURNAL OF CATALYSIS 151, 192–203 (1995)

Silica–Alumina-Supported Mo Oxide Catalysts: Genesis and Demise of Brønsted–Lewis Acidity

S. Rajagopal, J. A. Marzari, and R. Miranda[1]

Department of Chemical Engineering, University of Louisville, Louisville, Kentucky 40292

Received April 28, 1994; revised September 19, 1994

Diffuse reflectance FTIR spectroscopy of chemisorbed pyridine was used to investigate the influence of catalyst composition and treatment on the content of Brønsted and Lewis acidity. This investigation included oxidic and reduced Mo oxide catalysts containing 2, 4, 8, and 12 wt% MoO_3. The supports were seven silica–aluminas of composition between 0 and 100 wt% SiO_2. The IR spectra were collected at 200°C under helium flow, and the areas under the 1545 and 1450 cm^{-1} absorbance bands were related to the concentration of Brønsted and Lewis acid sites, respectively. The results indicate that the ratio of Brønsted to Lewis acid concentration (B/L) increases with SiO_2 content in the support and reaches a maximum for $SiO_2:Al_2O_3 = 75:25$ wt%. For Al_2O_3 and alumina-rich supports B/L increases continuously with MoO_3 loading because of the generation of new Brønsted acid sites and decrease of Lewis acid sites. For silica-rich supports, the B/L has a maximum at 2 wt% MoO_3 and then decreases slightly as MoO_3 loading is increased. The SiO_2 support with MoO_3 loading up to 12 wt% does not contain any Brønsted acidity in water-free environment. Upon reduction of the supported catalysts at 500°C in hydrogen, the B/L ratio decreases irrespective of SiO_2 content and MoO_3 loading. A structural model that includes tetrahedral surface species of Mo oxide explains the results. © 1995 Academic Press, Inc.

INTRODUCTION

High selectivity is usually provided to a catalyst by the compounding of two or more functionalities on the same material. Hydrogenolysis activity combined with acidity is one such set of functions that is often required. Reduced transition metal oxides, such as Mo oxides used in hydrotreatment catalysts, can yield those two functions by proper combination with an acidic support. In contrast to supported metal catalysts, in which the functions are uncoupled, the transition metal oxide component can provide both acidity and hydrogenolysis activity. Thus, knowledge of how much acidity is added to the catalyst by the transition metal oxide in the working state of oxidation is of utmost importance to the catalyst designer or user. In this paper we discuss how the amount and type of acidity in Mo oxide catalysts can be varied as a function of the loading and state of oxidation of the oxide, and of the composition of the amorphous silica–alumina support. Although related work has already appeared in the literature, this is the first comprehensive study of the subject mentioned; it includes a wide range of MoO_3 loading (2, 4, 8, and 12 wt%) and silica–alumina composition (0, 10, 25, 50, 75, 90, and 100 wt% SiO_2).

Kiviat and Petrakis (1) were the first to report the generation of Brønsted acidity by supporting MoO_3 on Al_2O_3. They also identified two types of Lewis acid sites (weak and strong) present on Al_2O_3 and supported MoO_3. Both types of acidity survived the reduction with hydrogen (1, 2). Moné and Moscou (3) and Moné (4) observed Brønsted and Lewis acidity on both hydrated and calcined MoO_3/Al_2O_3 and in $CoMo/Al_2O_3$, and noticed an increase in acidity upon calcination at 600°C. Ratnasamy and Knözinger (5) and Martínez and Mitchell (6) also reported the presence of Lewis and Brønsted acidic sites on MoO_3/Al_2O_3 and $CoMo/Al_2O_3$, as did Schrader and Cheng (7) and Riseman *et al.* (8). Segawa and Hall (9) and others (10, 11) showed that the generated Brønsted acidity could be eliminated by reduction in hydrogen. Kataoka and Dumesic (12) found both Lewis and Brønsted acid sites on unsupported MoO_3 and on >6.4 wt% MoO_3/SiO_2, whereas they found only Lewis sites in the range 1–6.4 wt% MoO_3/SiO_2. Although sulfided catalysts are beyond the scope of this paper, it is important to note that the effect of sulfidation on the acidity of MoO_3/Al_2O_3 has led to conflicting reports. Several authors (4, 5, 8, 10) have claimed the absence of Brønsted acidity on sulfided catalysts, while others (13) claim their presence. Recently, Topsøe *et al.* (14) also succeeded in finding Brønsted acid sites on sulfided catalysts.

The present paper reports on the acidic properties of oxidic and reduced Mo oxides supported on silica–aluminas as characterized by FTIR of chemisorbed pyridine. A new structural model explaining the appearance and disappearance of acidity is also presented.

[1] To whom correspondence should be addressed. E-mail: r0mira01@ulkyvm.louisville.edu.

0021-9517/95 $6.00

EXPERIMENTAL

Catalysts

The synthesis of supports and catalysts has been described in detail before (15). Briefly, Al_2O_3 was prepared by adding NaOH solution to a $Al(NO_3)_3 \cdot 9H_2O$ (Fisher) solution, which was then neutralized and precipitated with HNO_3. The silica–aluminas ($SiO_2 : Al_2O_3$ weight ratios = 10:90, 25:75, 50:50, 75:25, and 90:10) were prepared according to established techniques (16) from gelled $Na_2SiO_3 \cdot 9H_2O$ (Fisher) and $Al(NO_3)_3 \cdot 9H_2O$. SiO_2 was obtained from $Na_2SiO_3 \cdot 9H_2O$. All of the above solids were dried at 120°C for 4 h and calcined at 550°C for 12 h. The silica–alumina samples were ion exchanged three times with NH_4NO_3 and calcined further at 550°C. X-ray diffraction (XRD) of the powders revealed the amorphicity of SiO_2 and silica–aluminas containing ≥50 wt% SiO_2. The alumina support was confirmed to by γ-Al_2O_3. The content of γ-Al_2O_3 decreases with increasing SiO_2, becoming negligible in silica–aluminas with ≥50 wt% SiO_2.

Bulk unsupported MoO_3 was prepared by precipitation from an ethanolic solution of $(NH_4)_6Mo_7O_{24} \cdot 4H_2O$ (Alfa Products) (AHM), followed by calcination at 500°C for 12 h, according to a method proposed by Tsigdinos and Swanson (17).

Supported Mo oxide was prepared by incipient wetness (dry) impregnation of AHM. The loading of Mo oxide on each support was varied ranging from theoretical submonolayer to monolayer coverage (2, 4, 8, and 12 wt% MoO_3). For that purpose, the required concentration and volume of aqueous AHM, at a pH around 5.8, was added to the carrier at room temperature. The impregnated samples were left at room temperature for 2 h, dried at 120°C for 6 h, and calcined at 550°C for 12 h. The content of Mo in the calcined catalysts was verified by X-ray fluorescence spectroscopy. The nomenclature used for the supports and catalysts is given in Table 1.

Surface Area

BET surface areas of the 7 supports and 28 catalysts were determined by N_2 physisorption at −196°C using a conventional all-glass vacuum apparatus equipped with an electronic manometer (Datametrics).

Total Acidity

The total acidity of supports and catalysts, in their oxidized and reduced states, was determined by NH_3 chemisorption at 120°C in a temperature-programmed desorption apparatus. The detailed measurements have been described before (18).

Infrared Spectroscopy

A Perkin–Elmer 1720 FTIR with DTGS detector and KBr beam splitter was fitted with a diffuse-reflectance cell (Spectra-Tech 30-100) equipped with an environmental chamber (Fig. 1). The sample cup was usually loaded with about 10 mg of catalyst, loosely packed and flattened with a glass microscope slide. The FTIR instrument was typically operated at a scan speed of 0.1 cm^{-1} s^{-1} and a resolution of 4 cm^{-1}, collecting 100 scans per spectrum. The environmental chamber was utilized to treat the catalyst sample under vacuum, or gas flow, at a maximum temperature of 500°C. One thermocouple was located in the sample and another next to the heater. The latter was controlled to ±1°C with a PID controller (Omega CN9000). The gases (He and H_2) were purified by flowing through *oxygen trap* and molecular sieves (Alltech Associates) to remove oxygen and water, respectively. The gas and vacuum lines connected to the environmental chamber were heated stainless steel tubing of 1.6 mm OD, whose inside walls had been washed with methanolic KOH to reduce or eliminate adsorption of pyridine.

The oxidic catalysts were pretreated *in situ* at 500°C under He flow (5 ml min^{-1} NTP) for 1 h and cooled to

TABLE 1

Nomenclature of the Catalysts Used

Catalysts	Designation	Catalysts	Designation
γ-Al_2O_3	Al_2O_3	MoO_3(2 wt%)/Al_2O_3	M2Al[a]
SiO_2–Al_2O_3(10 : 90 wt%)	SA10	MoO_3(2 wt%)/SA10	M2SA10
SiO_2–Al_2O_3(25 : 75 wt%)	SA25	MoO_3(2 wt%)/SA25	M2SA25
SiO_2–Al_2O_3(50 : 50 wt%)	SA50	MoO_3(2 wt%)/SA50	M2SA50
SiO_2–Al_2O_3(75 : 25 wt%)	SA75	MoO_3(2 wt%)/SA75	M2SA75
SiO_2–Al_2O_3(90 : 10 wt%)	SA90	MoO_3(2 wt%)/SA90	M2SA90
SiO_2	SiO_2	MoO_3(2 wt%)/SiO_2	M2Si

[a] Similar designation is given to the 4, 8, and 12 wt% MoO_3 catalysts. Reduced catalysts are designated with the suffix R, e.g., M12AlR.

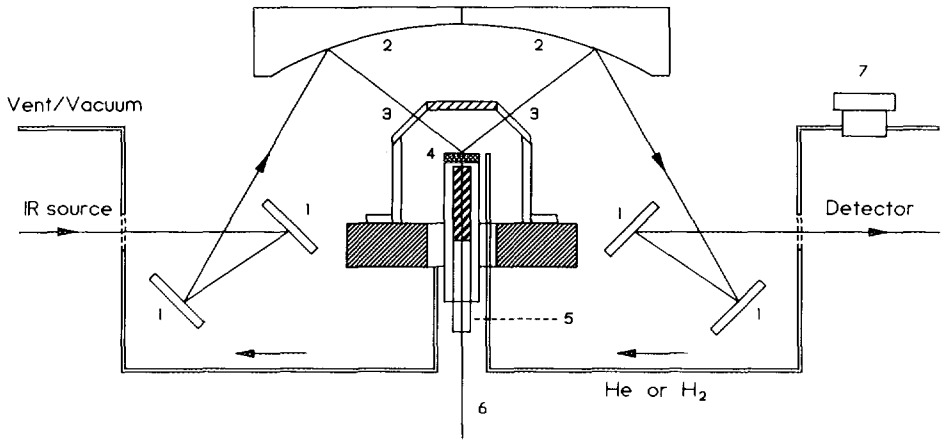

FIG. 1. Schematics of the diffuse reflectance cell with environmental chamber. 1, flat mirrors. 2, ellipsoidal mirrors. 3, CaF_2 windows. 4, sample. 5, heater. 6, thermocouple. 7, injector port.

200°C before recording a background spectrum. The reduced catalysts were prepared in two steps, in order to minimize the exposure of the environmental chamber windows to water vapor. First the oxidic catalysts were heated in H_2 (60 ml min^{-1} NTP) at 500°C for 2 h in a quartz reactor and cooled to room temperature. Then the prereduced samples were transferred to the environmental chamber and further reduced *in situ* at 500°C for 1 h (5 ml min^{-1} NTP of H_2). The sample was cooled to 200°C and H_2 flow was replaced by He before obtaining a background spectrum. Purified and molecular-sieve-dried pyridine was adsorbed on these samples at 200°C by injecting 2 μl upstream at room temperature. Typically all of the pyridine was carried over the catalyst with the He flow in less than 20 min. The infrared spectrum of chemisorbed pyridine was obtained at 200°C 1 h after injection, allowing enough time for the physisorbed/weakly chemisorbed pyridine to desorb from the catalyst.

The intensity under the bands at 1545 cm^{-1} (BPy) and 1450 cm^{-1} (LPy) was integrated between 1515 and 1565 cm^{-1} and between 1420 and 1470 cm^{-1}, respectively, using local baselines in these two ranges. The ratio of intensities of BPy to LPy bands was equated to the ratio of concentrations of Brønsted to Lewis acid sites, B/L. This procedure is justified in the Appendix.

RESULTS

Surface Area

BET surface areas of the supports and the oxidic catalysts are presented in Fig. 2. It is observed that loading of MoO_3 leads to a substantial loss (up to 27%) relative to the initial surface area of the support, particularly in the case of silica–aluminas. A likely cause for this loss is the formation of multilayers of octahedrally coordinated Mo, which could lead to restriction of the smallest micropores (15). Solid state reactions leading to new phases are not believed to be responsible for the diminishing surface areas.

Supports

Figure 3 shows the IR spectra of pyridine chemisorbed on silica–aluminas. The concentration of Brønsted acid sites, which is proportional to the area under the BPy band at 1545 cm^{-1}, increases with SiO_2 content, in agreement with the literature (19). Also the frequency of the LPy band (1450 cm^{-1}) increases with SiO_2 content, although that of the BPy band is invariant. The increase in frequency is due to increasing charge disturbance in the pyridine ring, resulting from chemisorption on stronger Lewis acid sites (see Discussion). Earlier findings on similar catalysts showed two different bands, corresponding to weak and strong Lewis acid sites (1). The presence of a single band in our case is due to the high temperature of chemisorption (200°C), which prevents adsorption of pyridine on the very weak acid sites. Additionally, it has

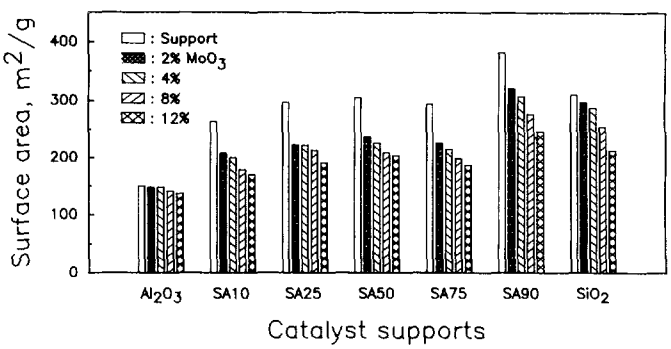

FIG. 2. BET surface areas of supports and Mo oxide catalysts.

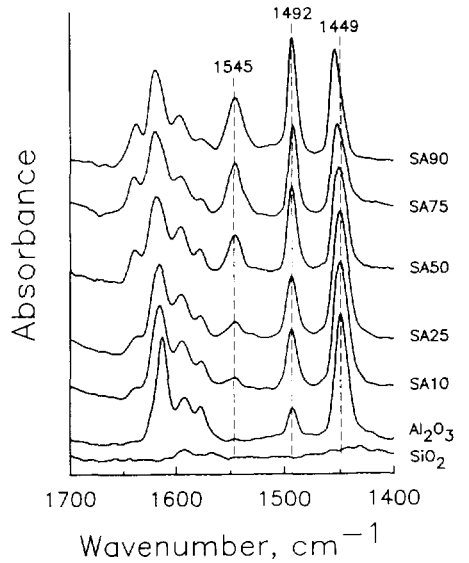

FIG. 3. FTIR spectra of chemisorbed pyridine on alumina, silica, and silica–aluminas at 200°C.

been reported that H-bonded pyridine is stable on SiO_2 at room temperature (20). Our results show no chemisorbed pyridine on SiO_2 at 200°C.

Oxidic Mo Oxide Catalysts

The spectra of pyridine chemisorbed on the oxidic catalysts are shown in Fig. 4. Similarly to the case of the silica–alumina carriers, the LPy band for the 2 wt% MoO_3 catalysts shifts to higher frequency at higher SiO_2 content. The shift diminishes as the loading of MoO_3 increases, an effect which will be explained under Discussion. The *B/L* ratio calculated from these spectra is plotted against the weight fraction of SiO_2 in Fig. 5, and against MoO_3 loading in Fig. 6. The *B/L* ratio increases with SiO_2 weight fraction and shows a maximum at 75 wt% SiO_2. It also increases when MoO_3 is added to all supports except SiO_2. It is of interest to examine the details of these results.

For Al_2O_3 carriers, Figs. 4–6 indicate that below 4 wt% MoO_3 no Brønsted acidity is present and that above that value new Brønsted acidity is generated in proportion to MoO_3 loading. This result substantiates the work of Kiviat and Petrakis, who observed Brønsted acidity on Al_2O_3 for loadings of MoO_3 above 6 wt% (1). In this work we show that alumina-rich carriers, such as SA10 and SA25, behave similarly to Al_2O_3 and differ in that they contain some Brønsted acidity before any MoO_3 is added. For carriers with intermediate content of Al_2O_3, such as SA50, a large increase in *B/L* ratio is observed at low loading of MoO_3, levelling off with further loading. For silica-rich carriers, such as SA75 and SA90, a 2 wt%

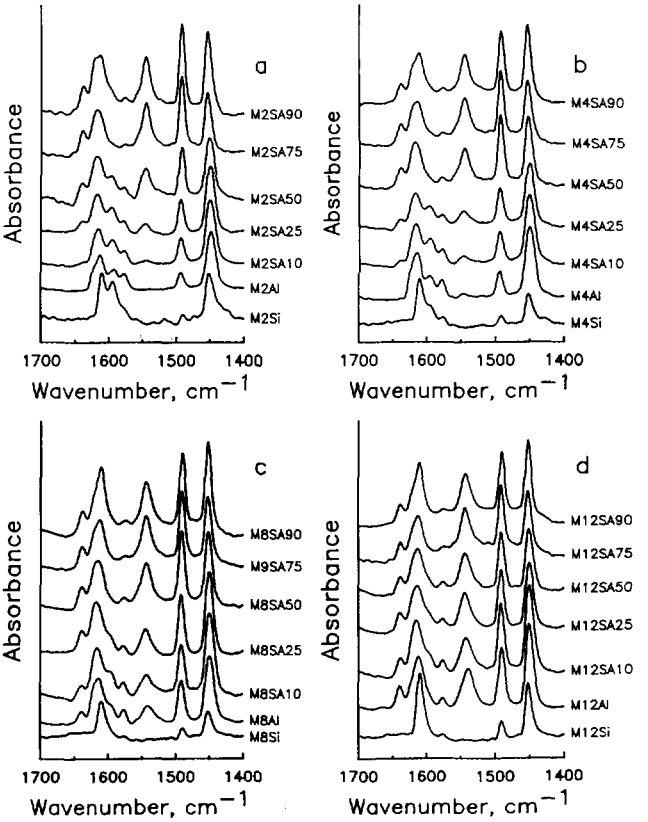

FIG. 4. FTIR spectra of chemisorbed pyridine on oxidic Mo oxide catalysts at 200°C. MoO_3 loading: (a) 2%, (b) 4%, (c) 8%, and (d) 12%.

loading of MoO_3 provokes an increase in *B/L* ratio, which decreases slightly with further loading.

Silica-supported catalysts show no Brønsted acidity,

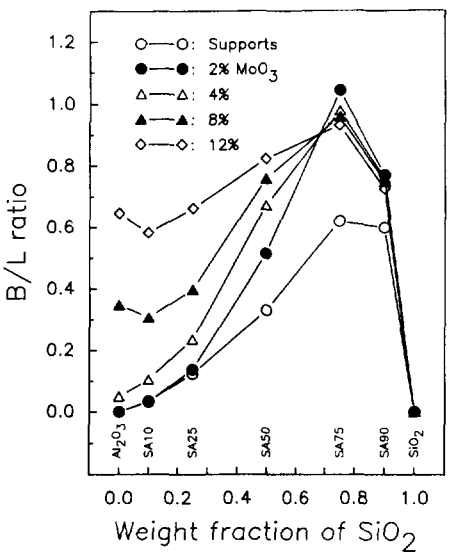

FIG. 5. Brønsted/Lewis acidity ratio for oxidic Mo oxide catalysts as a function of weight fraction of SiO_2.

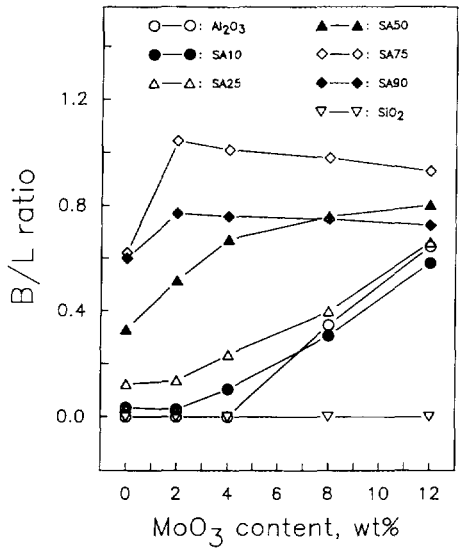

FIG. 6. Brønsted/Lewis acidity ratio for oxidic Mo oxide catalysts as a function of MoO_3 loading (wt%).

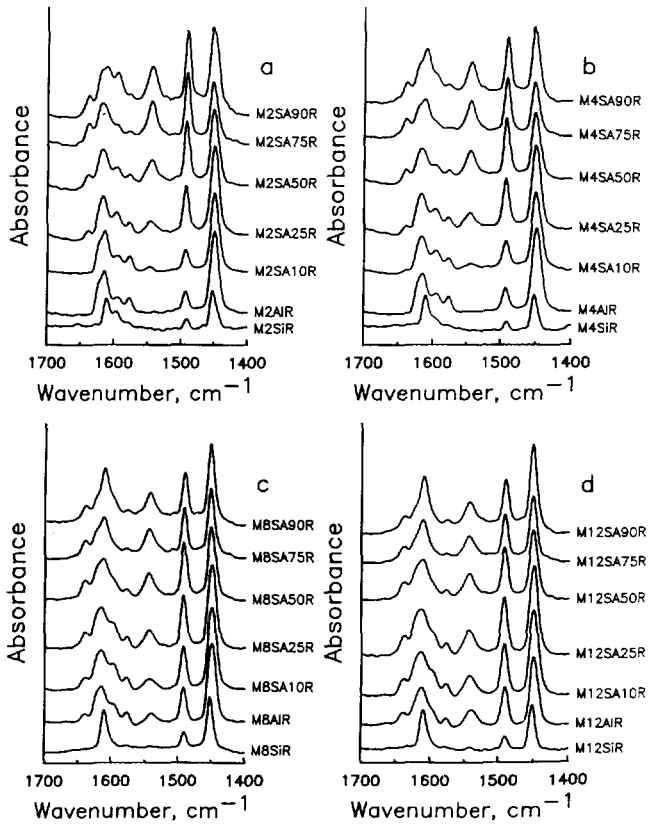

FIG. 7. FTIR spectra of chemisorbed pyridine on reduced Mo oxide catalysts at 200°C. MoO_3 loading: (a) 2%, (b) 4%, (c) 8%, and (d) 12%.

although they contain Lewis acidity. Upon introduction of water vapor into the environmental chamber, however, Brønsted acidity appears (the spectra are not shown). Earlier, Kataoka and Dumesic (12) observed only Lewis acid sites on 1 wt% MoO_3/SiO_2 and some Brønsted acidity on 6.4 wt% MoO_3/SiO_2; such Brønsted acidity may have been visible only when the sample was not completely dehydrated.

Reduced Mo Oxide Catalysts

Figure 7 depicts the IR spectra of pyridine chemisorbed on supported Mo oxide that has been reduced *in situ*. Figure 8 shows the corresponding *B/L* ratio as a function of weight fraction of SiO_2 in the support, and Fig. 9, the *B/L* ratio as a function of MoO_3 content. For most catalyst compositions, the process of reducing the Mo oxide provokes a decrease of the *B/L* ratio.

In the case of the Mo catalysts supported on Al_2O_3 and alumina-rich carriers ($SiO_2 \leq 50\%$), the *B/L* ratio of the reduced catalysts is higher than that of the corresponding supports. On the other hand, some of the catalysts supported on silica-rich carriers yield upon reduction *B/L* ratios that are below those of the corresponding supports. This is illustrated in Fig. 10, which compares the *B/L* ratios of supports to those of oxidic and reduced 12% MoO_3 catalysts. For weight fraction of SiO_2 above 50%, the *B/L* ratios of reduced catalysts are below those of the parent supports.

The significance of these changes can be clarified by considering the absolute acidity of selected compositions, as presented in Table 2. It must be noted that the absolute values of Brønsted and Lewis acidity reported there are calculated using a ratio of molar absorptivities of BPy to LPy bands equal to one.

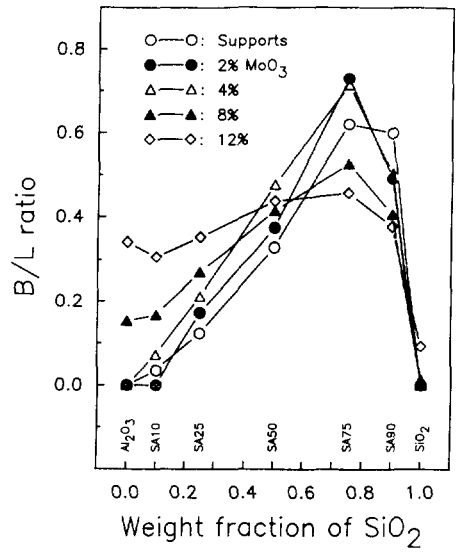

FIG. 8. Brønsted/Lewis acidity ratio for reduced Mo oxide catalysts as a function of weight fraction of SiO_2.

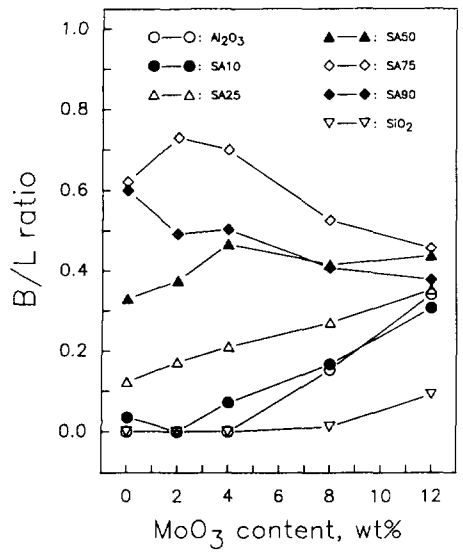

FIG. 9. Brønsted/Lewis acidity ratio for reduced Mo oxide catalysts as a function of MoO_3 loading (wt%).

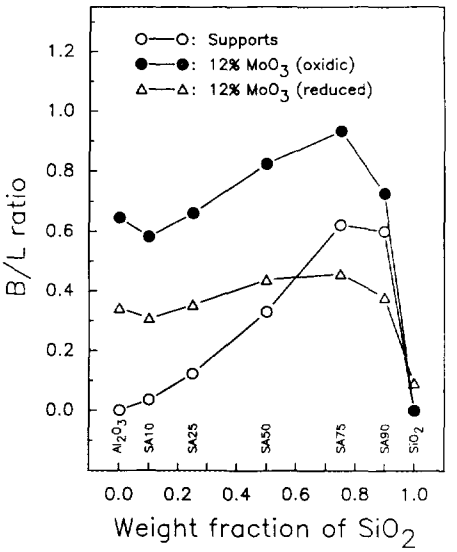

FIG. 10. Comparison of Brønsted/Lewis ratios of oxidic and reduced 12 wt% MoO_3 catalysts.

Examination of Table 2 reveals that upon loading with oxidic Mo, both SA25 and SA75 supports lead to generation of acidity, the increase being higher for the silica-rich catalyst. The new acidity is the result of the appearance of new Brønsted acid sites on SA25 and both Brønsted and Lewis on SA75. Upon reduction, the SA25 catalysts lose some of the Brønsted acidity generated, while the SA75 catalysts lose most or all of the new Brønsted and Lewis acidity.

These results are consistent with a structural model in which the new acidity resides on the surface of the deposited Mo oxide or at the exposed interface of Mo oxide

TABLE 2

Acidity of Selected Supports and Mo Oxide Catalysts[a]

	B/L	Total[b,c]	Brønsted[b]	Lewis[b,d]
Al_2O_3	0	0.30	0	0.30
2%MoO_3/Al_2O_3	0 → 0	0.32 → 0.31	0 → 0	0.32 → 0.31
4%MoO_3/Al_2O_3	0.04 → 0	0.33 → 0.32	0.01 → 0	0.32 → 0.32
8%MoO_3/Al_2O_3	0.34 → 0.15	0.33 → 0.31	0.08 → 0.04	0.25 → 0.27
12%MoO_3/Al_2O_3	0.65 → 0.34	0.37 → 0.29	0.15 → 0.07	0.22 → 0.22
SA25	0.12	0.51	0.05	0.46
2%MoO_3/SA25	0.13 → 0.16	0.52 → 0.52	0.06 → 0.07	0.46 → 0.45
4%MoO_3/SA25	0.22 → 0.21	0.54 → 0.52	0.10 → 0.09	0.44 → 0.43
12%MoO_3/SA25	0.65 → 0.35	0.61 → 0.50	0.24 → 0.13	0.37 → 0.37
SA75	0.62	0.27	0.10	0.17
2%MoO_3/SA75	1.04 → 0.73	0.37 → 0.30	0.19 → 0.13	0.18 → 0.17
4%MoO_3/SA75	0.96 → 0.71	0.41 → 0.28	0.20 → 0.12	0.21 → 0.16
12%MoO_3/SA75	0.94 → 0.46	0.50 → 0.22	0.24 → 0.07	0.26 → 0.15
12%MoO_3/SiO_2	0 → 0.09	0.29 → 0.10	0 → 0.01	0.29 → 0.09

[a] The arrows indicate the acidity before and after reduction: oxidic → reduced.

[b] Total, Brønsted, and Lewis acidities are expressed in equivalents of mmol NH_3/g catalyst.

[c] Total acidity obtained from Ref. (18).

[d] Brønsted and Lewis acidity calculated from *B/L* and Total = *B* + *L*.

and support. As Mo is deposited, new Lewis and Brønsted acid sites on the Mo oxide are generated while Lewis and Brønsted acid sites of the support are consumed. Thus it is possible that, after reduction of the oxide and consequent loss of some of its associated acid sites, the remanent acidity may be less than the original amount in the support.

Unsupported MoO_3

The synthesized orthorhombic MoO_3 has a BET surface area of 3.2 $m^2\ g^{-1}$, a total acidity of 0.034 mmol g^{-1}, and a B/L ratio of 0.15. Belokopytov *et al.* (21) and Kataoka and Dumesic (12) have also shown that MoO_3 contains both Brønsted and Lewis acidity. Upon reduction at 500°C, we found as well that the bulk product (which is MoO_2, as confirmed by XRD) exhibits negligible total acidity (0.005 mmol g^{-1}) that is only of the Lewis type ($B/L = 0$).

DISCUSSION

A brief description of the known acidic properties of γ-Al_2O_3, SiO_2, and silica–alumina supports will be given. This will be followed by a deeper examination of the causes for the observed changes of catalyst acidity that occur after loading and reducing Mo oxide.

It has been established that the surface of γ-Al_2O_3 contains only Lewis acid sites, as measured by the adsorption of pyridine or NH_3, although some evidence of Brønsted acidity that is not strong enough to protonate pyridine has also been given (22, 23). This Brønsted acidity is not expected to be catalytically active in most industrial reactions and was not detected in our IR spectra. The strong Lewis acid sites consist of oxygen vacancies or coordinatively unsaturated sites (cus) of Al.

SiO_2 is acidic, but too weak to chemisorb pyridine at 200°C under helium flow, as pointed out in this paper. This result agrees with our previous work showing that SiO_2 does not chemisorb NH_3 at 120°C under helium flow (25), and with Salama and Yamaguchi's work establishing that the TPD of pyridine from SiO_2 occurs with a T_{max} of 110°C (24). On the other hand, SiO_2 is able to physisorb H-bonded pyridine, but only at room temperature (20).

Silica-alumina has well-known Brønsted and Lewis acidity that increases with SiO_2 content (19, 26). The relevant questions to be considered, however, are how the deposited Mo oxide generates additional acidity and how the reduction process diminishes it. To answer these questions we will refer to established knowledge of the microstructure of supported Mo oxide.

Let us first focus on Mo oxide/Al_2O_3 prepared by incipient wetness impregnation. A monolayer structure for Mo oxide has been proposed (27) to be composed of Mo species with both tetrahedral and octahedral coordinations. The tetrahedral species are presumably formed in the initial stages of the reaction of basic OH groups of Al_2O_3 with MoO_4^{2-} and $Mo_7O_{24}^{6-}$ anions present in the impregnating solution, according to

$$8\ Al_sOH^- + Mo_7O_{24}^{6-} \rightarrow 4\ (Al_s)_2MoO_4 + 3\ MoO_4^{2-} + 4\ H_2O,$$

in which s denotes a surface species. The octahedral species are formed after the most basic OH groups of Al_2O_3 have been consumed, allowing the less basic, neutral, and acidic OH groups to react with the $Mo_7O_{24}^{6-}$ anions. Octahedral species also form during drying and calcination of the Mo ions that are not strongly bound to the Al_2O_3, or that, having remained in solution, precipitate on the Al_2O_3. The monolayer Mo oxide structure is shown by TPR and spectroscopic measurements, suggesting that for MoO_3 loading up to ca. 4 wt% a large fraction of Mo is highly dispersed and mostly tetrahedrally coordinated (15). For higher loading, the proportion of multilayers of Mo oxide increases quickly, as deduced from the increased reducibility of the oxide (15). In this paper we are showing that Brønsted acidity appears at $\geq$4 wt% MoO_3, coinciding with the appearance of multilayers of Mo oxide. The large Lewis acidity of Al_2O_3 is not decreased by the deposition of up to 4 wt% MoO_3 (see Table 2), and in fact is slightly increased. Higher content of MoO_3 causes the Lewis acidity to decrease and the Brønsted acidity to increase.

These observations on Lewis acidity can be explained by a surface model in which at low loading the tetrahedrally coordinated molybdate species do not occupy Al cus. This is justifiable on the basis that the molybdate may react strongly by forming bidentate species with pairs of adjacent surface hydroxyls (Scheme 1, Species I). However, at higher loadings we can not rule out the anchoring of molybdate anions by reaction with a hydroxyl and an adjacent Al cus (Scheme 1, Species II); evidence exists that Mo species are able to react with Al cus (28). This type of anchoring would lead to a decrease in the Lewis acidity, as observed for loadings higher than 4 wt%.

The generation of Brønsted acid sites following Mo oxide deposition has been observed before. Hall (29) proposed that the molybdate anions could impart Brønsted acidity to the adjacent Al_2O_3 hydroxyls. By this mechanism, however, we would expect Brønsted acidity to occur even at loadings lower than 4 wt%, contrary to our observations. Henker *et al.* suggested that heteropolymolybdates, which are solid acids, are formed on high-silica silica–aluminas (30). We advance that the newly created Brønsted acidity is associated with the multiple layers of octahedrally coordinated amorphous Mo oxide.

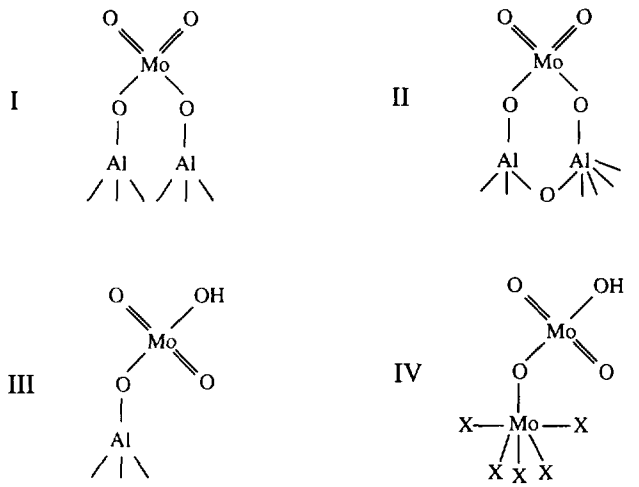

SCHEME 1. Cluster models of the tetrahedral molybdate species proposed to exist on alumina and Mo oxide surfaces. These models are derived from the formal reaction of a MoO_4^{2-} anion and the most abundant types of hydroxyls identified and classified by Knözinger and Ratnasamy (59): (I) two adjacent hydroxyls type Ia; (II) a Lewis site originating from a hydroxyl type IIa; (III) a hydroxyl type Ia; (IV) a hydroxyl on the surface of a slab of corner-shared Mo octahedra, in which X represents a unit of octahedrally coordinated Mo.

Crystalline MoO_3 does not lead to significant generation of Brønsted acidity; our results with bulk MoO_3 reveal that a small amount of Brønsted acidity is present, which is completely removed upon reduction. Such complete loss does not occur in the case of alumina-supported Mo oxide.

We speculate that Brønsted acid sites are formed at loadings $\geq$4 wt% on Al_2O_3 by the appearance of acidic surface species in the following way. At these loadings of MoO_3, the density and basicity of the unoccupied hydroxyls of Al_2O_3 are small. Therefore during impregnation the MoO_4^{2-} anions react with Al_2O_3 hydroxyls forming mainly monodentate species (Scheme 1, Species III) that are very acidic since they are products of reaction of strong acids with weakly basic hydroxyls. This speculation is supported by evidence presented of similar monodentate tetrahedral species in the case of WO_3/Al_2O_3 (31). Simultaneously with the formation of Species III, it is possible that monodentate groups also appear on top of the multiple layers of amorphous Mo oxide, leading to acidic Species IV (Scheme 1).

Let us now refer to MoO_3/SiO_2. The surface of SiO_2 support, unlike Al_2O_3, contains hydroxyl groups which are weakly basic or neutral, thus the deposited Mo oxide does not interact strongly and leads to three-dimensional oxide agglomerates upon calcination. These oxides have an orthorhombic MoO_3 X-ray structure which disappears after reduction with hydrogen (15). Our data show that all the generated acidity upon deposition of Mo oxide is of Lewis type and that the amount of new acidity generated per gram of catalyst is the highest in the group (Table 2). For example, 12 wt% MoO_3/SA75 generates 0.50 − 0.27 = 0.23 mmol g^{-1}, while 12 wt% MoO_3/SiO_2 produces 0.29 − 0 = 0.29 mmol g^{-1} (in NH_3 equivalents). These differences in types and amounts of acidity are related to the differences in surface structures of Mo oxide on these various supports. The Lewis acidity observed on the silica-supported catalysts must necessarily reside on the orthorhombic MoO_3 and is believed to be formed by coordinatively unsaturated sites of Mo (oxygen vacancies) on the surface of the crystallites.

The lack of Brønsted acidity in the oxidic silica-supported catalysts contrasts the abundant Brønsted sites formed on others supports. In terms of our surface model, it appears that the crystalline MoO_3 present on the silica support does not lead to the formation of the acidic Species IV. Ogata *et al.* (32) also affirm that calcined 8 wt% MoO_3/SiO_2 exhibits no Brønsted acidity at 100°C. However, it must be noted that admission of water over the SiO_2 catalysts induces trace amounts of Brønsted acidity. A possible cause is the appearance of silicomolybdic acid at the interface and edges of the Mo oxide crystallites. This phase has indeed been detected with several spectroscopic techniques on MoO_3/SiO_2 in the presence of water (32–36).

Next let us refer to the acidity characteristics of Mo oxide supported on silica–aluminas. All silica–aluminas contain a certain amount of isomorphous substitution of Si by Al, leading to the observed Brønsted acidity in the support. Silica–aluminas with less than 50 wt% SiO_2 (SA10 and SA25) consist of a silica–alumina phase dispersed in a continuous Al_2O_3 phase (characterized as γ-Al_2O_3 by XRD). They have a high content of Lewis acidity per gram, in fact more than γ-Al_2O_3 itself (Table 2), and resemble Al_2O_3 in their behavior toward binding of Mo oxide. Low loading (up to 2 wt% MoO_3) does not affect the Lewis acidity, while higher loading causes the acidity to decrease. The previously described model of Lewis acidity for alumina-supported catalysts applies here as well. The initial 2 wt% MoO_3 is bound to the support by reaction with strongly basic hydroxyls forming Species I. However, since the concentration of basic hydroxyls is smaller in SA10 (or SA25) than in Al_2O_3 because of the diluting effect of SiO_2, the onset of new Brønsted acidity and decrease in Lewis acidity on SA10 (or SA25) occurs at lower MoO_3 loading than on Al_2O_3. The reduction of Lewis acidity is produced by the formation of Species II and the appearance of new Brønsted acidity may be related, as in the case of Al_2O_3, to the formation of monodentate Species III. At higher loading of Mo oxide, multilayers of amorphous polymolybdates give rise to additional Brønsted acidity (Species IV), as previously described.

Silica–aluminas with more than 50 wt% SiO_2 (SA75 and SA90) appear to have a complex local structure according to Schreiber and Vaughan (37). On the one hand, there is the proper silica–alumina phase. In addition, it has been shown that calcination produces the displacement of a large fraction of aluminum ions from their framework position (38, 39), leading to the generation of a highly dispersed Al_2O_3 phase which may be the origin of most of the observed Lewis acidity. Moreover, a dispersed SiO_2 phase may be initially present or may originate during calcination. The heterogeneity of this kind of support gives rise to a variety of Mo oxide species (15) and, consequently, acidic characteristics. The absence of dense populations of basic hydroxyls and Al cus forces most of the initially deposited Mo oxide to be anchored as monodentate Species III, which generates new Brønsted acidity and does not decrease the Lewis acidity (see SA75 series in Table 2). As the Mo loading increases, multilayers of polymolybdates are generated using the monodentate species as anchors to the support (thus more Brønsted acidity as Species IV appears). Simultaneously, crystalline Mo oxide (identified as orthorhombic MoO_3 with XRD) is formed on the SiO_2 phase. This crystalline oxide was shown above to produce additional Lewis acidity in the form of Mo cus. In accordance, Table 2 shows that Lewis acidity for the SA75 series increases with MoO_3 content, contrary to what was observed on Al_2O_3 or low-silica silica–aluminas.

Effect of Support Composition on the Strength of Lewis Acidity

The observed IR shift toward higher frequency for the LPy band as SiO_2 content increases denotes a higher strength of Lewis acidity. This observation is consistent with other results in the literature. Leonard *et al.* (40) showed that the ratio tetrahedral/octahedral Al in silica–aluminas increases with SiO_2 content. Additionally, Connell and Dumesic (41) noted that pyridine adsorbed on tetrahedral Al give a band at 1624 cm^{-1} whereas those on octahedral Al cations absorb at 1612 cm^{-1}, proving that pyridine chemisorbs more strongly on tetrahedral Al than on octahedral Al. This was also shown with quantum chemical calculations by Knözinger (42). Therefore, the high-frequency shift of the LPy band is due to the increasing ratio of tetrahedral/octahedral Al in silica–aluminas of increasing SiO_2 content. In the present work it is noted that the shift in the LPy band observed for the silica-supported Mo oxide catalysts is not as large as for the alumina-supported catalysts. It may be inferred then that pyridine is chemisorbed less strongly on Mo cus than on Al cus. No independent literature result confirming this speculation was found.

Effect of Reduction of Mo Oxide on Catalyst Acidity

Total acidity is in general diminished upon reduction, mostly for the highly loaded, high-silica-content silica–aluminas. However, it is useful to view the details of how acid sites are lost, in the framework of the surface acidity model proposed in this paper.

Previous studies have shown that the reducibility of tetrahedrally coordinated Mo species is much smaller than that of multilayered or crystalline Mo oxide (15). Thus is is not surprising that the acidity (Brønsted or Lewis) of alumina-supported catalysts is less affected than that of silica-supported catalysts (Table 2). According to our model, there is also another reason for those differences. In the Al_2O_3 catalysts the Lewis sites are mostly located on the support itself, which is not reducible. Therefore, even for 8 and 12 wt% MoO_3/Al_2O_3, the Lewis acidity does not change in going from oxidic to reduced catalyst. The Brønsted acid sites, on the other hand, are affected because the monodentate Species IV anchored to the multilayered oxide suffer a reduction from Mo^{+6} to Mo^{+4} and thus lose their acidity. Note that not all Brønsted acidity is lost. This is a consequence of the incomplete reduction of the monodentate Species III anchored to the support directly.

The silica-supported catalysts undergo a different mechanism of loss of acidity. They contain Lewis acid sites which are located on the Mo oxide. Upon reduction of Mo^{+6} to Mo^{+4}, there is a structural transformation from MoO_3 to a denser MoO_2-type structure which provokes the loss of Mo cus (and thus Lewis acidity) and the appearance of Mo–Mo metal bonds. In fact, the existence of metal–metal bonds in MoO_2 is well established (43) and has been reported to occur also in reduced supported Mo oxide catalysts (44).

The silica-alumina catalysts resemble to some extent the alumina- or silica-supported catalysts. For alumina-rich catalysts (SA10 or SA25), Lewis acidity of the oxidic form is not significantly lost upon reduction, while Brønsted acidity is partially lost but remains at a level above that of the parent support. On silica-rich catalysts (SA75 and SA90) the Lewis acidity is noticeably lost in going from oxidic to reduced form, for the same reasons as the SiO_2 catalysts. The Brønsted acidity in silica-rich catalysts is lost to a larger extent than in alumina-rich catalysts because of the larger proportion of multilayered Mo oxide. For the 12 wt% MoO_3/SA75, for example, the remaining Brønsted acidity is even smaller than for its parent support SA75.

CONCLUSIONS

Data were presented on the characterization of the acidity of a complete series of Mo oxide loaded to various

extent on a set of silica–aluminas from 0 to 100% SiO_2. Quantitative evaluation of pyridine chemisorption bands LPy and BPy yielded curves of Brønsted/Lewis ratio as a function of catalyst composition, for oxidic and reduced Mo oxide. These figures constitute a reference for the design of Mo oxide/silica–aluminas with specified amount and type of acidity.

The generation of new acid sites upon deposition of Mo oxide on various supports could be explained by a model of surface structure that agrees with current knowledge. The same model was able to explain the total or partial destruction of such new acid sites when the oxide is reduced. Mo oxide deposition on Al_2O_3 and alumina-rich supports provokes the loss of Lewis acid sites by reaction with Al cus. No further loss of Lewis acidity occurs upon reduction of those catalysts. The deposited Mo oxide also generates Brønsted acid sites which are apparently associated with tetrahedral Mo species strongly bound in a monodentate manner to Al in the support or to Mo in a polymolybdate layer. Reduction of the oxide affects mostly the layered species and thus the Brønsted acidity of those catalysts containing a large fraction of polymolybdate layers. Crystalline MoO_3, which appears mainly on silica-rich supports, leads to the generation of Lewis acid sites associated with Mo cus. Reduction of the oxide causes crystalline rearrangement, loss of Mo cus, and thus of Lewis acidity.

TABLE 3

Assignment of Infrared Absorption Bands of Adsorbed Pyridine[a]

Vibration mode	PPY[b] (cm^{-1})	HPy[c] (cm^{-1})	LPy[d] (cm^{-1})	BPy[e] (cm^{-1})
8a[f] $\nu_{CC(N)}$	1580	1614	1620,1595	1638
8b $\nu_{CC(N)}$	1593	1572	1577	1620
19a $\nu_{CC(N)}$	1490	1482	1490	1490
19b $\nu_{CC(N)}$	1438	1439	1450	1545

[a] Adapted from Ref. (48).
[b] Physically adsorbed pyridine.
[c] Pyridine adsorbed via hydrogen bonding.
[d] Pyridine adsorbed on Lewis acid sites.
[e] Pyridine adsorbed on Brønsted acid sites.
[f] Nomenclature proposed by Kline and Turkevich (49). 8a and 19a modes are assigned to the totally symmetrical vibrations, whereas 8b and 19b are assigned to the antisymmetric vibrations in the plane of the molecule.

APPENDIX

Quantitative Analysis by Infrared Diffuse Reflectance

The theory of infrared diffuse reflectance from powders was developed by Kubelka and Munk (45, 46) and relates the concentration of scatterer to the intensity of scattered radiation. For an infinitely thick layers, the Kubelka–Munk (KM) function $f(R_\infty)$ may be expressed as

$$f(R_\infty) = (1 - R_\infty)^2/2R_\infty = k/s,$$

where R_∞ is the ratio of diffuse reflectance of the scattering species to that of the nonabsorbing material in which the species is dispersed, k is the molar absorption coefficient, and s is the scattering coefficient. For dilute samples in low-absorbing or nonabsorbing matrices, it has been established that $k = 2.303\varepsilon c$, where ε is the molar absorptivity and c is the molar concentration of the ana-

TABLE 4

Relative Molar Absorptivities of Infrared Absorption Bands of Adsorbed Pyridine

$\varepsilon^L_{1450}/\varepsilon^B_{1545}$	$\varepsilon^B_{1490}/\varepsilon^L_{1490}$	$\varepsilon^L_{1490}/\varepsilon^L_{1450}$	$\varepsilon^B_{1490}/\varepsilon^B_{1545}$	Ref.	Year
8.8	1.0	—	—	(50)	1964
—	6.0 ± 0.9	0.25	—	(51)	1966
1.08 ± 0.09	5.8	0.17	—	(52)	1967
1.1	—	—	—	(53)	1968
1.54	5.2	—	—	(54)	1971
1.0 ± 0.04[a]	—	—	0.63 ± 0.02	(1)	1973
0.9 ± 0.1	—	—	—	(55)	1980
—	2.74	—	3.5	(56)	1984
0.925[b]	—	—	—	(11)	1985
—	1.0	0.207	—	(57)	1987
1.32[c]	—	—	—	(58)	1993

[a] This ratio was obtained for η-Al_2O_3 using only the stronger Lewis acid bands. The corresponding ratio for the weaker Lewis acid bands was 1.40 ± 0.04.
[b] This ratio was determined for η-Al_2O_3 using the stronger Lewis acid bands. For the weaker bands the value obtained was 1.80. For MoO_3/Al_2O_3, the measured values were 0.788 and 1.22, respectively.
[c] This ratio was obtained for silica–alumina-supported catalysts, at 150°C.

lyte (47). Therefore,

$$f(R_\infty) = 2.303\varepsilon c/s = k'\varepsilon c.$$

Assuming a small specular reflection component and a constant scattering coefficient (which depends on particle size and size distribution), the KM function is proportional to the concentration of analyte, and in this manner diffuse reflectance can be used for quantitative analysis. Our instrument does not directly yield reflectance in KM units, but in absorbance units, which are equivalent to −log(reflectance), and thus the spectral intensities are proportional to concentration in the following manner:

$$-\log(\text{reflectance}) = \text{absorbance} \propto \varepsilon c.$$

Table 3 gives representative assignments of absorption bands observed for chemisorbed pyridine (48). The concentration of acid sites is typically measured from the 19b bands: Brønsted acid sites yield a band at 1545 cm^{-1} (BPy), and Lewis acid sites one at 1450 cm^{-1} (LPy). The ratio of intensities is equal to $\varepsilon^{B}_{1545}c^{B}/\varepsilon^{L}_{1450}c^{L}$; thus, calculation of B/L requires values of $\varepsilon^{B}_{1545}/\varepsilon^{L}_{1450}$. Table 4 gives previously reported values (1, 11, 50–58) of $\varepsilon^{L}_{1450}/\varepsilon^{B}_{1545}$, which vary between 0.75 and 1.54 (except for a single value of 8.8). Since there is no agreement in the literature, we have arbitrarily taken $\varepsilon^{B}_{1545}/\varepsilon^{L}_{1450} = 1$, and so the ratio of concentrations of Brønsted to Lewis acid sites is equal to the ratio of integrals of BPy to LPy absorbance bands.

ACKNOWLEDGMENTS

Financial support from DOE (Grant DE-FG22-89PC89771), NSF (Grant RII-8610671), and the Commonwealth of Kentucky (EPSCoR Office) is greatly appreciated.

REFERENCES

1. Kiviat, F. E., and Petrakis, L., *J. Phys. Chem.* **77,** 1232 (1973).
2. Fransen, T., van der Meer, O., and Mars, P., *J. Phys. Chem.* **80,** 2103 (1976).
3. Moné, R., and Moscou, L., *in* "Hydrotreating and Hydrocracking," ACS Symp. Ser. 20, p. 150. ACS, Washington, DC, 1975.
4. Moné, R., *in* "Preparation of Catalysts" (B. Delmon, P. A. Jacobs, and G. Poncelet, Eds.), p. 381. Elsevier, Amsterdam, 1976.
5. Ratnasamy, R., and Knözinger, H., *J. Catal.* **54,** 155 (1978).
6. Martínez, N. P., and Mitchell, P. C. H., *in* "Proceedings, 3rd Climax Int. Conf. Chem. and Uses of Molybdenum" (H. F. Barry and P. C. H. Mitchell, Eds.), p. 105. Climax Molybdenum, Ann Arbor, MI, 1979.
7. Schrader, G. L., and Cheng, C. P., *J. Phys. Chem.* **87,** 3675 (1983).
8. Riseman, S. M., Bandyopadhyay, S., Massoth, F., and Eyring, E. M., *Appl. Catal.* **16,** 29 (1985).
9. Segawa, K., and Hall, W. K., *J. Catal.* **76,** 133 (1982).
10. Valyon, J., Schneider, R. L., and Hall, W. K., *J. Catal.* **85,** 277 (1984).
11. Suarez, W., Dumesic, J. A., and Hill, C. G., *J. Catal.* **94,** 408 (1985).
12. Kataoka, T., and Dumesic, J. A., *J. Catal.* **112,** 66 (1988).
13. Tanaka, K., and Okuhara, T., *in* "Proceedings, 3rd Climax Int. Conf. Chem. and Uses of Molybdenum" (H. F. Barry and P. C. H. Mitchell, Eds.), p. 170. Climax Molybdenum, Ann Arbor, MI, 1979.
14. Topsøe, N. -Y., Topsøe, H., and Massoth, F. E., *J. Catal.* **119,** 252 (1989).
15. Rajagopal, S., Marini, H., Marzari, J. A., and Miranda, R., *J. Catal.*, **147,** 417 (1994).
16. Magee, J. S., and Blazek, J. J., *in* "Zeolite Chemistry and Catalysis" (J. A. Rabo, Ed.), ACS Monograph Vol. 171, p. 615. ACS, Washington, DC, 1976.
17. Tsigdinos, G. A., and Swanson, W. W., *Ind. Eng. Chem. Prod. Res. Dev.* **17,** 208 (1978).
18. Rajagopal, S. Marzari, J. A., and Miranda, R., submitted for publication.
19. Schwarz, J. A., Russell, B. G., and Harnsberger, H. F., *J. Catal.* **54,** 303 (1978).
20. Parry, E. P., *J. Catal.* **2,** 371 (1963).
21. Belokopytov, Yu. V., Kholyavenko, K. M., and Gerei, S. V., *J. Catal.* **60,** 1 (1979).
22. Peri, J. B., *J. Phys. Chem.* **69,** 231 (1965).
23. Dunken, H., and Fink, P., *Z. Chem.* **5,** 432 (1965).
24. Salama, T. M., and Yamaguchi, T., *in* "Acid–Base Catalysis (K. Tanabe, H. Hattori, T. Yamaguchi, and T. Tanaka, Eds.), p. 289. Proceedings International Symposium on Acid–Base Catalysis, Sapporo, Japan, 1988.
25. Rajagopal, S., Grimm, T. L., Collins, D. J., and Miranda, R., *J. Catal.* **137,** 453 (1992).
26. Benesi, H. A., and Winquist, B. H. C., *Adv. Catal.* **27,** 97 (1978).
27. Massoth, F. E., *Adv. Catal.* **27,** 265 (1979).
28. van Veen, J. A. R., Hendriks, P. A. J. M., and Andrea, R. R., *J. Phys. Chem.* **94,** 5275 (1990).
29. Hall, W. K., *in* "Proceedings, 4th Climax Int. Conf. Chem. and Uses of Molybdenum" (H. F. Barry and P. C. H. Mitchell, Eds.), p. 224. Climax Molybdenum, Golden, CO, 1982.
30. Henker, M., Wendlandt, K.-P., Valyon, and J., Bornmann, P., *Appl. Catal.* **69,** 205 (1991).
31. Bernholc, J., Horsley, H. A., Murrell, L. L., Sherman, L. G., and Soled, S., *J. Phys. Chem.* **91,** 1526 (1987).
32. Ogata, A., Kazusaka, A., Yamazaki, A., and Enyo, M., *Chem. Lett.* **1,** 15 (1989).
33. Castellan, A., Bart, J. C. J., Vaghi, A., and Giordino, N., *J. Catal.* **42,** 162 (1976).
34. Chumachenko, N. N., Yurieva, T. M., Tarasova, D. V., and Aleshina, G. I., *React. Kinet. Catal. Lett.* **14,** 87 (1980).
35. Marcinkowska, K., Rodrigo, L., Roberge, P. C., and Kaliaguine, S., *J. Mol. Catal.* **33,** 189 (1985).
36. Stencel, J. M., D'Este, J. R., Markovsky, L. E., Rodrigo, L., Marcinkowska, K., Adnot, A., Roberge, P. C., and Kaliaguine, S., *J. Phys. Chem.* **90,** 4739 (1986).
37. Schreiber, L. B., and Vaughan, R. W., *J. Catal.* **40,** 226 (1975).
38. Müller, D., Starke, P., Jank, M., Wendlandt, K. -P., and Bremer, H., *Z. Anorg. Allg. Chem.* **517,** 167 (1984).
39. Henker, M., Wendlandt, K.-P., Shapiro, E. S., and Tkachenko, O. P., *Appl. Catal.* **61,** 353 (1990).
40. Leonard, A., Suzuki, S., Fripiat, J. J., and De Kimpe, C., *J. Phys. Chem.* **68,** 2608 (1964).
41. Connell, G., Dumesic, J. A., *J. Catal.* **102,** 216 (1986).
42. Knözinger, H., *in* "Catalysis by Acids and Bases" (B. Imelik, C. Naccache, G. Goudurier, Y. B. Taarit, and J. C. Vedrine, Eds.), p. 111. Elsevier, Amsterdam, 1985.
43. Baird, M. C., *in* "Progress in Inorganic Chemistry," Vol. 9, p. 28. Interscience, New York, 1968.

44. Weigold, H., *J. Catal.* **83,** 85 (1983).
45. Kubelka, P., and Munk, F., *Z. Tech. Phys.* **12,** 593 (1931).
46. Kubelka, P., *J. Opt. Soc. Amer.* **38,** 448 (1948).
47. Kortum, P., Braun, W., and Herzog, G., *Angew. Chem., Int. Ed. Enl.* **2,** 333 (1963).
48. Ward, J. W., *in* "Zeolite Chemistry and Catalysis" (J. A. Rabo, Ed.), ACS Monograph Vol. 171, p. 118. ACS, Washington, DC, 1976.
49. Kline, C. H., Jr., and Turkevich, J., *J. Chem. Phys.* **12,** 300 (1944).
50. Basila, M. R., Kantner, T. R., and Rhee, K. H., *J. Phys. Chem.* **68,** 3197 (1964).
51. Basila, M. R., and Kantner, T. R., *J. Phys. Chem.* **70,** 1681 (1966).
52. Hughes, T. R., and White, H. M., *J. Phys. Chem.* **71,** 2192 (1967).
53. Ward, J. W., *J. Catal.* **11,** 271 (1968).
54. Lafrancois, M., and Malbois, G., *J. Catal.* **20,** 350 (1971).
55. Matulewicz, E. R. A., Kerkhof, F. R. J. M., Moulijn, J. A., and Reitsma, H. J., *J. Colloid Interface Sci.* **77,** 110 (1980).
56. Sayed, M. B., Kydd, R. A., and Cooney, R. P., *J. Catal.* **88,** 137 (1984).
57. Rosenthal, D. J., White, M. G., and Parks, G. D., *AIChE J.* **33,** 336 (1987).
58. Emeis, C. A., *J. Catal.* **141,** 347 (1993).
59. Knözinger, H., and Ratnasamy, P., *Catal. Rev.* **17,** 31 (1978).